Received: 25 February 2020 | Revised: 7 March 2020 | Accepted: 17 March 2020

DOI: 10.1002/inf2.12119

REVIEW ARTICLE

WILEY

Anisotropic polaritons in van der Waals materials

Weiliang Ma[1,3] | Babar Shabbir[2] | Qingdong Ou[2] | Yemin Dong[3] | Huanyang Chen[4] | Peining Li[1] | Xinliang Zhang[1] | Yuerui Lu[5] | Qiaoliang Bao[2,3]

[1]Wuhan National Laboratory for Optoelectronics

[2]Department of Materials Science and Engineering, ARC Centre of Excellence in Future Low-Energy Electronics Technologies (FLEET), Monash University, Clayton, Victoria, Australia

[3]State Key Laboratory of Functional Materials for Informatics, Shanghai Institute of Microsystem and Information Technology, Chinese Academy of Sciences, Shanghai, China

[4]School of Electronic Science and Engineering, Xiamen University, Xiamen, Fujian Province, China

[5]Research School of Electrical, Energy and Materials Engineering, the Australian National University, Canberra, Australian Capital Territory, Australia

Correspondence
Qiaoliang Bao, Department of Materials Science and Engineering, ARC Centre of Excellence in Future Low-Energy Electronics Technologies (FLEET), Monash University, Clayton, VIC 3800, Australia.
Email: qiaoliang.bao@gmail.com

Funding information
Australian Research Council, Grant/Award Numbers: IH150100006, CE170100039; China Postdoctoral Science Foundation, Grant/Award Number: 2017M622758, LHTD20170006

Abstract

Polaritons in two-dimensional (2D) materials continues to garner significant attention due to their favorable ability of field-confinement and intriguing potential for low-loss and ultrafast optical and photonic devices. The recent experimental observation of in-plane anisotropic dispersion in natural van der Waals materials has revealed much richer physics as compared to isotropic plasmonic materials, which provides new insight to manipulate the polaritons and manufacture flat optical devices with unprecedented controls. Herein, we give an overview of the recent progress in in-plane anisotropic polaritons launched and visualized in the near-field range in 2D layered van der Waals materials. Furthermore, future prospects in this promising but emerging field are featured on the basis of its peculiar applications. This review article will stimulate the scientific community to explore other hyperbolic materials and structures in order to develop optical technologies with novel functionalities and further improve the understanding of the exotic photonic phenomena.

KEYWORDS

hyperbolic materials, in-plane anisotropy, optical and photonic devices, polaritons, scanning near-field optical microscopy

1 | INTRODUCTION

Polaritons—collective excitations formed by the coupling of photons with oscillating charges—in van der Waals materials provide a new way to manipulate light at nanoscale. Until now, various types of polaritons in van der Waals crystals, including those formed by free electrons (plasmon polaritons),[1-5] strongly-bound electron-hole pairs (exciton-polaritons),[6-8] and bound lattice vibrations (phonon polaritons [PhPs])[9-11] have been discovered and already shown promising potentials in light-based technologies beyond diffraction limit spanning a broad range of the electromagnetic spectrum.[12,13] Among these polaritons, PhPs with hyperbolicity attracted significant attention due to their strong field confinement, low losses, and long lifetimes.[14] Basically, the nature of light propagating inside a medium can be described by the dielectric permittivity tensor (ε = diag [ε_x, ε_y, ε_z]) at such frequency, where ε_x, ε_y are the in-plane components and ε_z is the out-of-plane component. [15] Many distinctive and non-intuitive optical phenomena associated with polaritons require negative perimittivity.[16,17] The peculiar properties of light propagation in a medium stem from the isofrequency surface in the momentum space, which are defined by the sign of $\varepsilon_i(i = x, y, z)$. When the medium is crystallographically anisotropic, it will hold different dielectric responses along different directions. If one of the permittivities, that is, $\varepsilon_i(i = x, y, z)$, is opposite in sign to the other two components, such medium then exhibits hyperbolicities,[18,19] which are the key to a range of sub-diffractional optical phenomena, such as negative refraction,[20,21] hyperlens,[22-24] nanolithography,[25,26] and enhancement of quantum radiation.[27] Furthermore, when $\varepsilon_x * \varepsilon_y < 0$,the hyperbolicities can also exist in the planar surface.[28,29]

Theoretically, the polaritons propagate along the layers with an in-plane anisotropic dispersion in case of different permittivities along orthogonal in-plane directions. The polaritons show an elliptic in-plane dispersion, subject to different permittivities but with the same signs whereas; for different signs, the polaritons possess an in-plane hyperbolic dispersion. The prominent example of hyperbolic natural material is hexagonal boron nitride (hBN).[9,14] The hBN is a polar van der Waal material with uniaxial permittivities possessing two mid-infrared Reststrahlen bands, one of which spans from 1395 to 1630 cm^{-1} (for the case of enriched hBN), where $\varepsilon_x = \varepsilon_y = \varepsilon_\perp < 0$ (the in-plane permittivity is negative and isotropic) and $\varepsilon_z = \varepsilon_\parallel > 0$ (the out of plane permittivity is positive).[23,24,30] Therefore, the PhPs in hBN show an out-of-plane hyperbolic dispersion and isotropic in-plane dispersion.[23,24,28,31,32] Although the PhPs with in-plane hyperbolic dispersion can be induced in nanostructured hBN (ie, artificial metamaterial), its visualization in natural materials was highly desirable.[33] Recent discovery of anisotropic polariton propagation along the surface of a natural vdW α-MoO_3 flakes demonstrates PhPs with elliptic and hyperbolic in-plane dispersion,[34,35] promise substantial advances in the fields of infrared optics and nanophotonics.[36] Contrary to artificial metamaterials with delicate designs, anisotropic polaritons in natural vdW materials with in-plane hyperbolic dispersions could manipulate light with unprecedented controls especially with subdiffractional confinement, low losses, and polarization sensitivities.[4,34]

In this review, we summarize the recent progress of planar anisotropic polaritons on their near-field responses with an emphasis on the natural layered materials, which may exhibit more potentials than conventional metasurfaces at some frequency ranges with critical applications. Firstly, we introduce the real-space nanoimaging mechanism by using scattering-type scanning near-field optical microscopy (s-SNOM) and summarize the research progress of polaritons in 2D materials. The basics of anisotropic polaritons with hyperbolic/elliptic dispersions are then discussed. After briefly reviewing the hyperbolic metasurfaces, we focus on the natural layered system for in-plane anisotropy and present several potential applications taking advantage of its unique abilities to control light. This review is aimed at providing a timely overview of the potential development of naturally hyperbolic media in novel optical devices. It is extremely attractive that naturally in-plane anisotropic materials may thus establish a new paradigm in nanophotonics, promising an unprecedented potential for the directional control of light and light-matter interactions at the nanoscale.

2 | DIRECT VISUALIZATION OF POLARITONS IN REAL SPACE

Polaritonics provides a unique way to harness, guide, and manipulate light at nanoscale much smaller than the diffraction limit.[37] Initially, surface plasmon polaritons in metals set an early stage for investigating this distinctive branch of optics.[38-40] However, the loss associated with electron/plasma scattering and interband transitions is unacceptably large.[41,42] The emergence of 2D materials offers new opportunities to explore low-loss polaritons compared with metal plasmonics. The development of the real-space nanoimaging technique has allowed us to directly observe these highly confined polaritons in the near field and conveniently study the fundamental physics of low-dimensional materials.[12,13]

Featuring a wavelength-independent nanoscale spatial resolution (~10 nm, determined by the diameter of the tip apex), s-SNOM provides deterministic observations and characterizations of various polaritons in real space.[43] As an important visualization technique, it shows an exceptional capability of unfolding quantum phenomena.[1,9,33,34,44,45] Specifically, infrared (IR) light is focused onto a high-frequency oscillating metallic tip of an atomic force microscope. The tip functions as an optical antenna that effectively generates optical near-fields with wave vectors much larger than that of the incident light, which thus can match the excitation conditions of the polaritons in the materials of interest. Generally, the propagating properties and the wavelength of a polariton can be extracted from the local optical field and periodicity of the interference fringes in s-SNOM images.[1,2] The dispersion relation of the polariton is thus attainable, along with the quantitative measure of the propagation loss from the real-space imaging. A detailed review of the development of the s-SNOM technique can be found in a reference by Chen et al.[43] Hyperspectral imaging by the nanoscale Fourier transform infrared (nano-FTIR) spectroscopy can also offer the nanometer spectral and spatial resolution to study polaritonic behaviors as the tip is raster-scanned over the sample (line-scans), which is often employed as

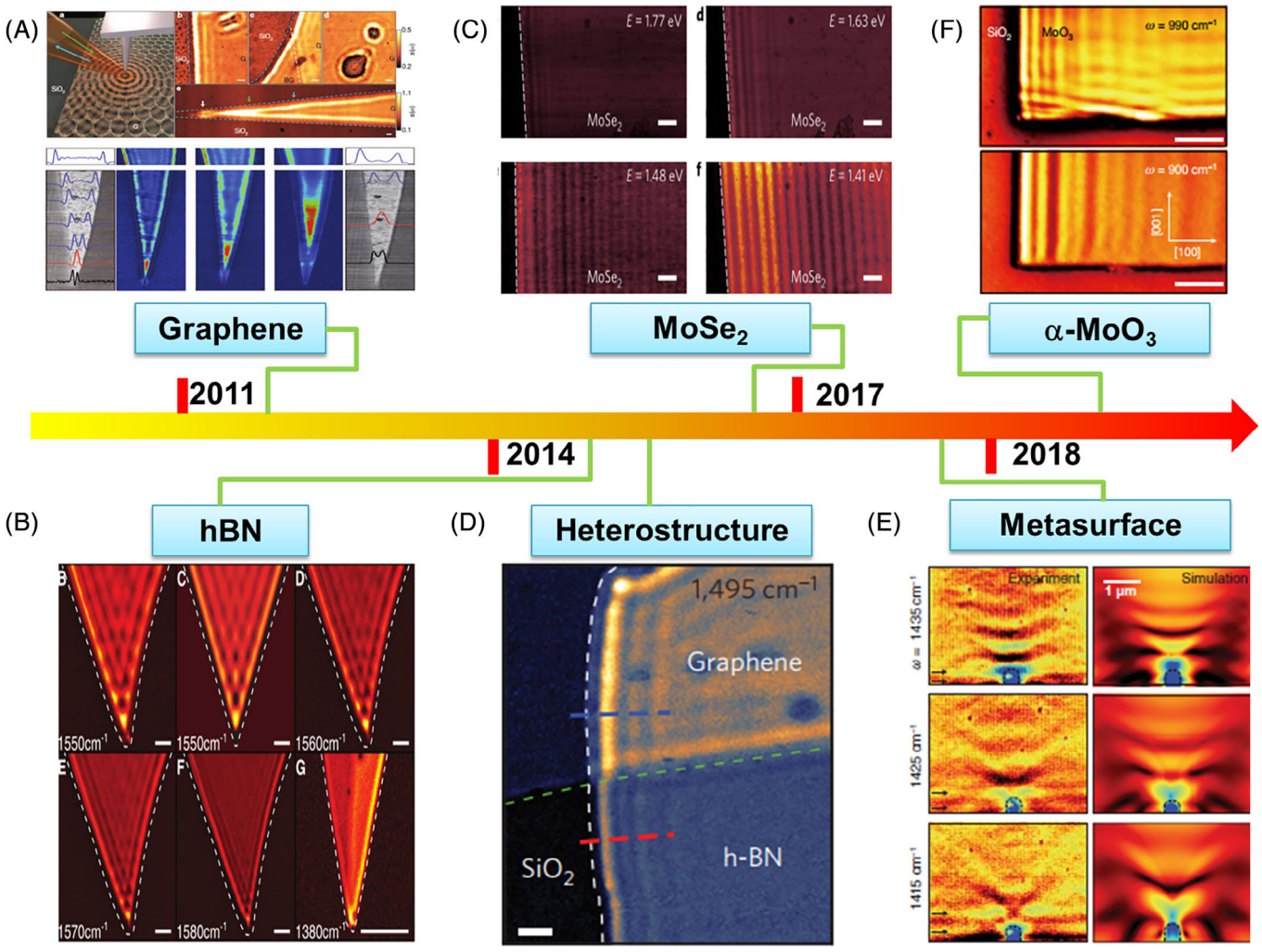

FIGURE 1 The roadmap of investigating polaritons in two-dimensional (2D) materials. A, s-SNOM image of graphene plasmon-poalriton.[1,2] Reproduced with permission from Reference 1, 2 copyright 2011, Nature Publishing Group. B, s-SNOM image of PhPs in hBN.[9] From Reference 9 reprinted with permission from AAAS. C, s-SNOM image of exciton-polariton waveguide modes in $MoSe_2$.[6] Reproduced with permission from Reference 6 copyright 2017, Nature Publishing Group. D, The atomic-scale photonic hybrids by heterostructures.[49] Reproduced with permission from Reference 49 copyright 2015, Nature Publishing Group. E, In-plane hyperbolic polaritons on metasurface.[33] From Reference 33 reprinted with permission from AAAS. F, In-plane anisotropic polaritons in natural materials of MoO_3.[34] Reproduced with permission from Reference 34 copyright 2018, Nature Publishing Group. hBN, hexagonal boron nitride; s-SNOM, scattering-type scanning near-field optical microscopy

a powerful tool complimentary to monocharmatic single-frequency imaging by the s-SNOM.[46-48]

By utilizing s-SNOM, Chen et al[1] and Fei et al[2] (independently) demonstrated the real-space imaging of the polaritonic waves in graphene, in 2011, for the first time. Particularly, the strong light confinement, gate-tunability, and long lifetimes can be found in such an atomically thin layer (Figure 1A). Graphene plasmonics not only opens an avenue for applying plasmon polaritons in graphene into low-loss gate-tunable nanophotonic devices, but also inspires the discovery of potential polaritons in other 2D materials. PhPs in hBN, distinctive from plasmons in graphene, were observed by Dai and coworkers in 2014,[9] whereas these lattice-vibration-dependent PhPs can be sustained in hBN down to few layers (even monolayer in their recent study[50]). (Figure 1B). Polaritons with highly low losses can exist in hBN as volume-confined modes that stem from the large birefringence between in-plane and out-of-plane. Details will be discussed in the following parts. Different from the spectral investigation of strongly coupled cavity exciton-polaritons, Fei[7] and Hu et al[6] observed the real-space propagation of exciton-polariton waveguide modes in layered WSe_2 and $MoSe_2$ at room temperature (Figure 1C). The nano-optical imaging of exciton-polaritons clearly unveils the high sensitivity of the polariton propagation length to the excitation energy, with a large propagation length up to 12 μm allowing for long-range energy or information transfer in future nanophotonic circuits.

To overcome the limitations of the individual polaritons, atomic-scale photonic hybrids of van der Waals heterostructures provide an extra degree of freedom to tune these polaritons (Figure 1D).[49,51] For example, the graphene/hBN heterostructure supports a new form of hybrid plasmon-PhPs with a broad bandwidth range and long lifetime that can be actively controlled through electrical gates.[52-56] Recent observations of the anomalous propagation of polaritons on infrared hyperbolic surfaces uncovers the novel physics in these layered materials (Figure 1E,F).[33,34] The in-plane hyperbolic polaritons in both natural α-MoO_3 and nanostructured hBN metasurface show the great potential of squeezing infrared light with directional control and ultralow loss. Moire polaritons based on twisted 2D bilayers have also attracted significant interest recently, including the directed propagation control of surface plasmons in Moire graphene superlattice,[57] Moire excitons in twisted stacks of monolayer transition metal dicalcogenides[58] and phonon based soliton superlattices in twisted hBN.[59] Therefore, the study of polaritons in 2D materials is a vibrant area of research at the vanguard of materials science, engineering, physics, and biology, where anisotropic polaritons play a fascinating role in manipulating the nano-light with orientational selectivity (Table 1).

3 | BASICS OF ANISOTROPIC POLARITONS

As referred above, the nature of light propagating inside a medium can be described by the iso-frequency contour in the k-space. Briefly, the momentum k corresponding to each wavelength of polaritons can be defined by permittivities at constant ω. The dielectric permittivity is a frequency-dependent tensor (ε = diag [ε_x, ε_y, ε_z], where ε_x, ε_y are the in-plane components and ε_z is the out-of-plane component. If the permittivity tensors (along different axes) are of opposite signs, the medium is called hyperbolic materials.[9,10,15,18,19] The strong optical anisotropy will render a series of potential applications in nanophotonics including negative refraction, hyperlens, and enhanced quantum radiation.[68-73] Normally, hyperbolic media was often discussed in the context of metamaterials, which aim at the novel properties that are not attainable in a natural system by "meta-atom." The detailed review of this aspect can be referred to the reference by Alexander et al.[19] Recently, the bulk hyperbolicity was observed in the natural system—hBN, which has emerged as a new platform for investigating sub-diffractional imaging and focusing, ultraslow hyperbolic polariton propagation, negative group velocity, and the hybridization of two different classes of propagating polaritons.[11] Actually, many bulk hyperbolic materials has been identified in nature, such as graphite,[74] magnesium diboride,[75] quartz,[76] tetradymites,[77] calcite,[78] and α-Al_2O_3 single crystal.[79] However, both the hyperbolic metamaterials and naturally hyperbolic materials can be defined by the different signs of permittivity between in- and out-of-plane. Generally the polaritons supported by these mediums are in-plane isotropic, it is challenging to realize optical functionalities for particular orientations and polarization in the planar surface, which are essential for high-performance polaritonic applications such as imaging and energy transfer devices.[80,81]

In this part, we will focus on our main aspect of this review—in-plane anisotropic polaritons. Because of the 2D nature, we are more interested in the confined and propagating TM modes supported by anisotropic media. The dispersion of these polaritons can be defined by the following relation.[29,82-84]

$$\eta_0^2\left(k_x^2\sigma_{xx}+k_y^2\sigma_{yy}\right)^2\left(k_x^2+k_y^2-k_0^2\right)-4k_0^2\left(k_x^2+k_y^2\right)^2=0.$$

where $k_{x,y}$ is the in-plane wave vectors, $\sigma_{xx,\ yy}$ are the in-plane conductivity along x and y directions, $k_0 = 2\pi/\lambda_0$ is

TABLE 1 Real-space characteristics of polaritons in two-dimensional (2D) natural materials

Material	Polariton types	Tunability methods	Lifetime	Refs.
Graphene	• Plasmon polaritons • In-plane isotropic polaritons	• Gating • Doping • Dielectric environment • Photo excitation	Near 2 Ps	1-3,54,60
BP	• Plasmon polaritons • In-plane anisotropic polaritons	• Photo excitation	NG	5
hBN	• Phonon polaritons • Hyperbolic volume and surface polaritons • In-plane isotropic polaritons	• Thickness • Dielectric environment • Isotopic enrichment	Near 8 Ps	9,14,61-64
α-MoO_3	• Phonon polaritons • In-plane hyperbolic polaritons • In-plane elliptical polaritons	• Thickness • Metal atoms intercalation	Over 8 Ps	34,35,65
WSe_2	• Exciton polaritons • Waveguide modes • In-plane isotropic polaritons	• Thickness • Dielectric environment	NG	7,66
$MoSe_2$	• Exciton polaritons • Waveguide modes • In-plane isotropic polaritons	• Thickness • Dielectric environment	NG	6
MoS_2	• Waveguide modes • In-plane isotropic	• Thickness • Dielectric environment	NG	67

Note: Not including heterostructures here.
Abbreviations: BP, black phosphorus; hBN, hexagonal boron nitride; NG, not given.

the wave vector in free space. The features of wave propagation in in-plane anisotropic medium can be defined by the geometry of the iso-frequency contour in momentum space, which can also be referred by the Fourier transform of the wave propagation in real space (shown in Figure 2). We will begin with the in-plane field distribution to distinguish the different types of in-plane anisotropic media. Figure 2 shows the relationship of the in-plane z-component of the electric field and the relative sign of the real part of permittivities Re(ε) (or the imaginary part of conductivities Im(σ)). The well-known metallic surface plasmon polariton, graphene plasmons,[85] PhPs in hBN,[32,86] surface PhPs in SiC[87] are all the in-plane isotropic polaritons resulting in the circularly spreading in real space (shown in Figure 2A). The highly symmetrical propagation of polaritons cannot render precise control of in-plane energy transfer or polarization. The elliptical and hyperbolic shape of in-plane anisotropic field distribution (shown in Figure 2B-D) indicates the anisotropic propagation of polaritons with diverse k in a different direction. Notice that while in the elliptic case, the propagation along both x- and y- directions are permitted. In the hyperbolic case, the propagation along one of the axes is not allowed. Furthermore, the giant optical anisotropy will induce the in-plane hyperbolicity (shown in Figure 2C,D), the large-k polaritons are referred to open curve in momentum space, which will be used to enhance quantum radiation.

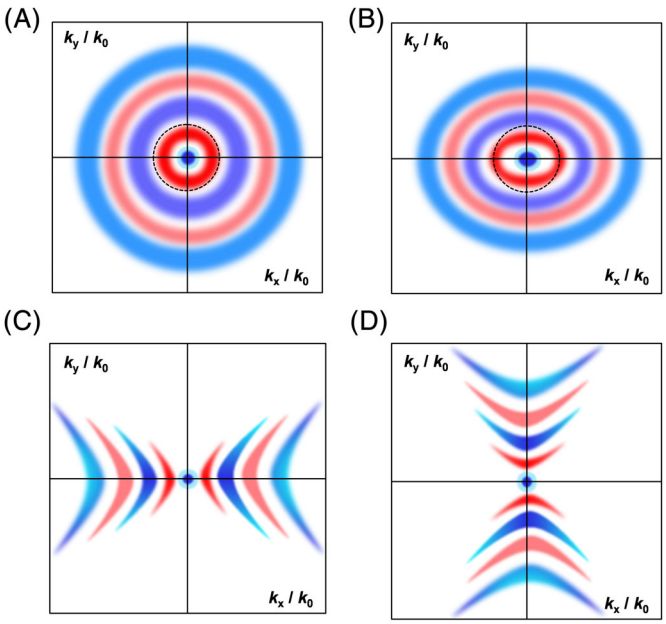

FIGURE 2 Field distribution excited by a z-directed dipole for different media. A, An in-plane isotropic media. B, An in-plane elliptic media ($\varepsilon_x * \varepsilon_y > 0$, $\varepsilon_x \neq \varepsilon_y$). C, An in-plane hyperbolic media ($\varepsilon_x < 0$, $\varepsilon_y > 0$). D, An in-plane hyperbolic media ($\varepsilon_x > 0$, $\varepsilon_y < 0$)

Moreover, because of their planar nature (in-plane), the optical devices based on them are readily integrated with other flat optical and optoelectronic elements.

4 | HYPERBOLIC METASURFACES

One effective way to achieve extremely large wave confinement and local density of states is to artificially reconstruct thin layers of an isotropic materials. Such manmade media can support the in-plane hyperbolic polaritons with ultra-high momentum. Through the manmade metallic gratings, one can drastically modified the dispersion of surface plasmons.[88] The periodic metallic gratings could support the propagation of surface polaritons with hyperbolic wavefront and orientational selectivity. The theoretical predictions have been readily verified in later experiments based on the hyperbolic metasurface of artificial silver/air gratings at visible frequency (see Figure 3A,B).[89] The device indicated clear planar negative refraction and diffraction-free propagation. The hyperbolic metasurface was also verified by anisotropic metallic arrays at microwave frequencies.[90] Gomez-Diaz et al showed the possible realizations of hyperbolic metasurface at terahertz using nanostructured graphene.[91] Very recently, Li et al demonstrated the infrared hyperbolic metasurface by nanostructuring hBN that supports highly confined anisotropic PhPs (see Figure 3C,D).[33] Compared with metallic surface plasmon polariton, the PhPs in hBN have notably low loss. By appropriately engineering the "meta-atoms," one may obtain different hyperbolic metasurfaces at some frequency ranges.[92] However, the noteworthy losses associated with plasmonic materials used in artificial hyperbolic surface and undesirable confinement at long wavelength range ($k_p \approx k_0$) could result in the unsatisfactory performance of optical devices. Moreover, the losses induced by fabrication imperfections are inevitable. The maximum momentum of propagating polaritons is determined by the inverse size of "meta-atom," the optical device will be cutoff when approaching this ultimate momentum. Although the hyperbolic mediums are also called indefinite materials because of the open curve of iso-frequency

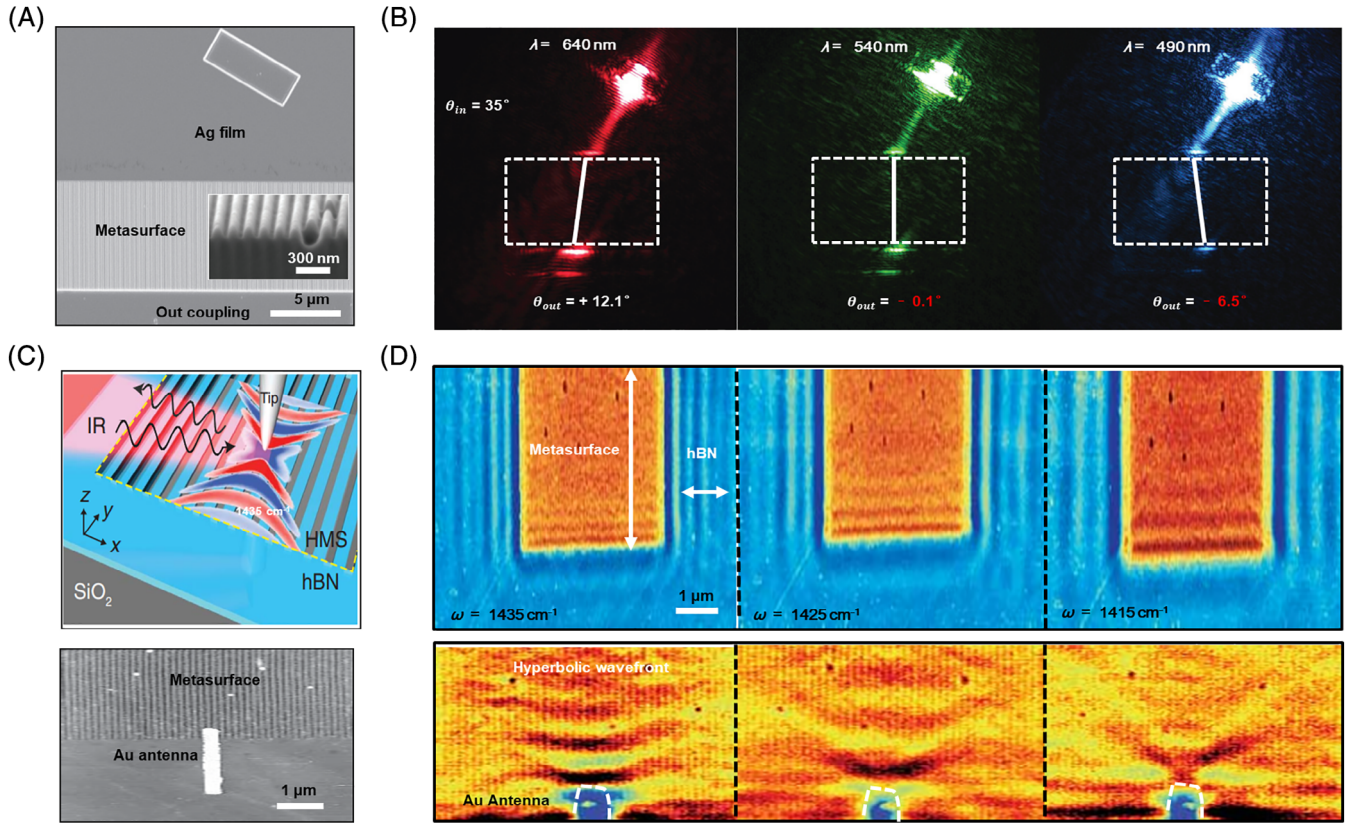

FIGURE 3 Artificial in-plane hyperbolic metasurfaces at visible and infrared frequency.[33,89] A, The planar negative refraction device at visible frequency. The inserted image indicates the surface plasmon based metasurface (Ag/air grating). B, Experimental demonstration of negative refraction on hyperbolic metasurfaces. The color plots show measurements of surface plasmons propagating along silver and being refracted at the interface with a hyperbolic metasurface (dashed box) implemented by nanostructured silver film. Reproduced with permission from Reference 89 copyright, Nature Publishing Group. C, infrared hyperbolic metasurface based on nanostructured hBN. D, Up: Polariton-interferometry imaging of PhPs on hyperbolic metasurface at infrared range. Bottom: Wavefront imaging of antenna-launched PhPs on hyperbolic metasurface. From Reference 33 reprinted with permission from AAAS. hBN, hexagonal boron nitride; PhPs, phonon polaritons

contour (ideally indefinite k), the metamaterials do not hold the key to the full potential of hyperbolic medium. Recently, it was demonstrated that some natural materials could offer advances in the realization of in-plane hyperbolic surface.[34,35] In particular, the natural α-phase molybdenum trioxide (α-MoO_3) and black phosphorus (BP), which have strong in-plane optical anisotropy, hold great promise for directional control of the polariton—propagation.

5 | NATURALLY IN-PLANE ANISOTROPIC POLARITONS

Since the discovery of graphene, research on various 2D materials has boomed in the fields of material science, chemistry, physics, biology, and nanotechnology.[93,94] Among the broad array of 2D materials, some in-plane anisotropic materials play important roles in optical and electronic applications.[12,13,68,95] The most striking feature of such 2D materials is the naturally high in-plane anisotropy of its macroscopic physical properties, which arises due to its special orthorhombic lattice. Here, we will review the progress on naturally anisotropic materials with a particular emphasis on α-MoO_3 and BP, and mainly focus on their advance in terms of in-plane anisotropic polaritons. As discussed above, the directional propagation of polaritons in the plane results from large in-pane optical anisotropy. The in-plane anisotropic media often support anisotropic polaritons (like Dyakonov surface wave).[96,97] Large optical anisotropy is generally found in structurally anisotropic materials, for example, strong birefringence or dichroism has been observed in biaxial crystals with orthorhombic structure. Among those materials, both α-MoO_3 and BP have interesting orthorhombic-layered structure.

The schematics of Figure 4A shows the crystal structure of α-MoO_3, where layers formed by distorted edge-shared MoO_6 octahedra are weakly bonded by van der Waals forces. The α-MoO_3 lattice constants a, b, and c, along the three directions in space (x, y, z) are all different. In each double layer structure, MoO_6 forms corner-sharing chains along the [001] direction and edge-sharing chains along the [100] direction (shown in Figure 4A). Three O atoms differently linked with one Mo atom, of which O_2-Mo is along the [001] direction and O_3-Mo along the [100] direction. The α-MoO_3 has a strong in-plane structure anisotropy as the difference of the spacing between (100) facets and (001) facets is as large as 7.2% Consequently, α-MoO_3 is a biaxial material with strong in-plane anisotropy. Similar to α-MoO_3, BP atomic layers are stacked together with van der Waals force while the single layer is bonded by sp^3 phosphorus atoms, as shown in Figure 4B. The BP layer-to-layer spacing is around 0.52 nm. As shown in side-view from different in-plane perspective, BP displays a strong in-plane anisotropy between the crystal orientations along "zigzag" and "armchair" directions.

The crystal structure of these two materials has conspicuous differences along two orthogonal directions in the plane. Consequently, the dielectric function is highly in-plane anisotropic resulting from variations in the real part of permittivity as a function of in-plane directions. It is noteworthy the strong in-plane anisotropy of permittivity at resonance frequencies can render directional propagation of polaritons. This indicates that natural α-MoO_3 and BP crystals can be the good candidates that support in-plane anisotropic polaritons so as to realize the natural hyperbolic surface. Besides, many theory works predicted the polaritons with in-plane directional propagation behavior in natural materials.[29,91,98-103] All of these in-plane anisotropic polaritons can be inherited by the different collective oscillations of electrons or optical phonons along different directions. The low in-plane lattice symmetry leads to distinct anisotropy.

One should note that the mechanisms of in-plane optical anisotropy in BP and α-MoO_3 are essentially different. In case of BP, the 2D description of anisotropic polaritons was based on its anisotropic conductivity.[4,99] The interplay between interband and intraband motions renders different oscillations of electrons—in-plane anisotropic plasmon polaritons, as illustrated in Figure 4D. Generally, if an antenna (metallic nanostructure) is used to launch the polaritons in polaritonic materials, the polaritons propagate away from the antenna as circular waves in many cases such as those in graphene, hBN, SiC, and so on. In BP, the inductive optical response along two in-plane axes enables the hyperbolic rays launched by an antenna.[29] If a z-oriented dipole emitter is used to launch the polaritons along homogeneous surface (as shown in Figure 5A-D), one can observe different polaritonic isofrequency contours while tuning the anisotropic conductivity. The hyperbolic plasmons and topological transitions can also be expected over the planar surface. In the highly anisotropic regime ($\mathrm{Im}\ \sigma_x * \sigma_y < 0$), the plasmon propagating along some direction are totally forbidden (shown in Figure 5E, F).[4,102] The dispersion relation imply that the resonance modes can be found only along x axis in some frequency regime (ie, above 0.47 eV), as presented in Figure 5E. The principal components of the conductivities in BP have opposite signs (Figure 5F, ie, $\sigma_{xx}\sigma_{yy} < 0$), which are the signatures for in-plane hyperbolic plasmon. There are a few ways to modulate the imaginary parts of BP conductivity, such as optical and chemical doping, so as to tune the in-plane anisotropy.[103-105] Although BP is a great

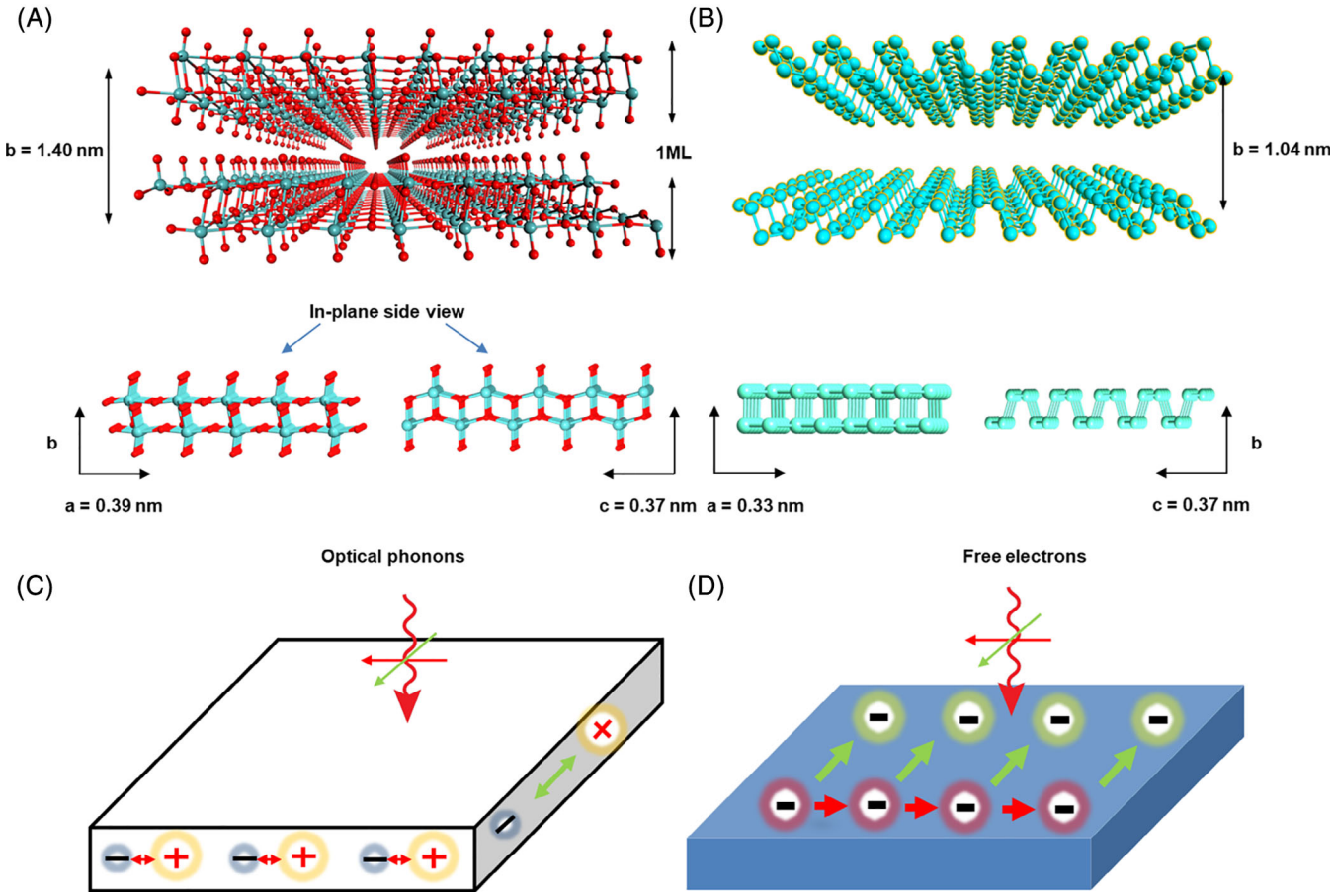

FIGURE 4 Lattice schematics of natural α-MoO_3 and black phosphorus (BP), schematic of the in-plane anisotropic collective oscillations of optical phonons and electrons. A, Up: Schematic illustration of the orthorhombic lattice structure in layered α-MoO_3 (blue spheres: molybdenum; red spheres: oxygen). The lattice constants of α-MoO_3 are B = 1.40 nm, A = 0.39 nm, and C = 0.37 nm. Bottom: The in-pane side view of the monolayer structure revealing in-plane anisotropic crystal structure defined in the A-B plane and C-B plane. B, Schematic illustration of the orthorhombic lattice structure in black phosphorus. C, Schematic illustrating the in-plane anisotropic collective oscillations of atomic displacements in the form of optical phonons in α-MoO_3. D, Schematic illustrating the in-plane anisotropic collective oscillations of free electrons in BP

candidate to investigate directional control of the propagation of plasmon polaritons,[100,106] the experimental observation of in-plane anisotropic polaritons propagating in BP has still remained elusive so far, due to the lack of suitable lasers as excitation mid/far-IR light coupled into s-SNOM. Recently, the theoretical studies on electromagnetic modes in biaxial slabs and accurate infrared anisotropic permittivities of α-MoO_3 were further developed.[107,108]

Another mechanism of optical in-plane anisotropy relies on highly discrete optical phonons. For polar crystal (eg, SiC and α-MoO_3), the anisotropic optical-phonons often result in multiple spectral ranges that are assigned to "Reststrahlen bands" (RBs),[109] resulting from a long-wavelength incident optical field in the resonance frequency range. The strength of resonances always shows a strong dependence on the polarization of the excitation beam, as illustrated in Figure 4C. For example, α-MoO_3, a polar van der Waals crystal, has received considerable attention over the past decade for nanoscale light-control because of strong birefringence in this material. Ma et al experimentally observed the low-loss hyperbolic and elliptical polaritons in natural α-MoO_3 crystals. In this work, novel in-plane hyperbola-type anisotropy in the form of hyperbolic PhPs, resulting from in-plane anisotropic dispersion, was reported. Utilizing high-resolution s-SNOM technique, the polariton interferometry images show strong direction-dependence, as revealed in Figure 6A-D.[34] Interestingly, the interference pattern in the upper-RB (U-RB) depicts an elliptical shape with the largest PhPs wavelength along the [001] surface direction, whereas it transforms into an almond shape in the lower-RB (L-RB) with the largest wavelength along the [100] direction. The Fourier transform analysis of Figure 6A,B gives an ellipsoid in the U-RB (Figure 6C) and hyperbola in the L-RB (Figure 6D), revealing that the

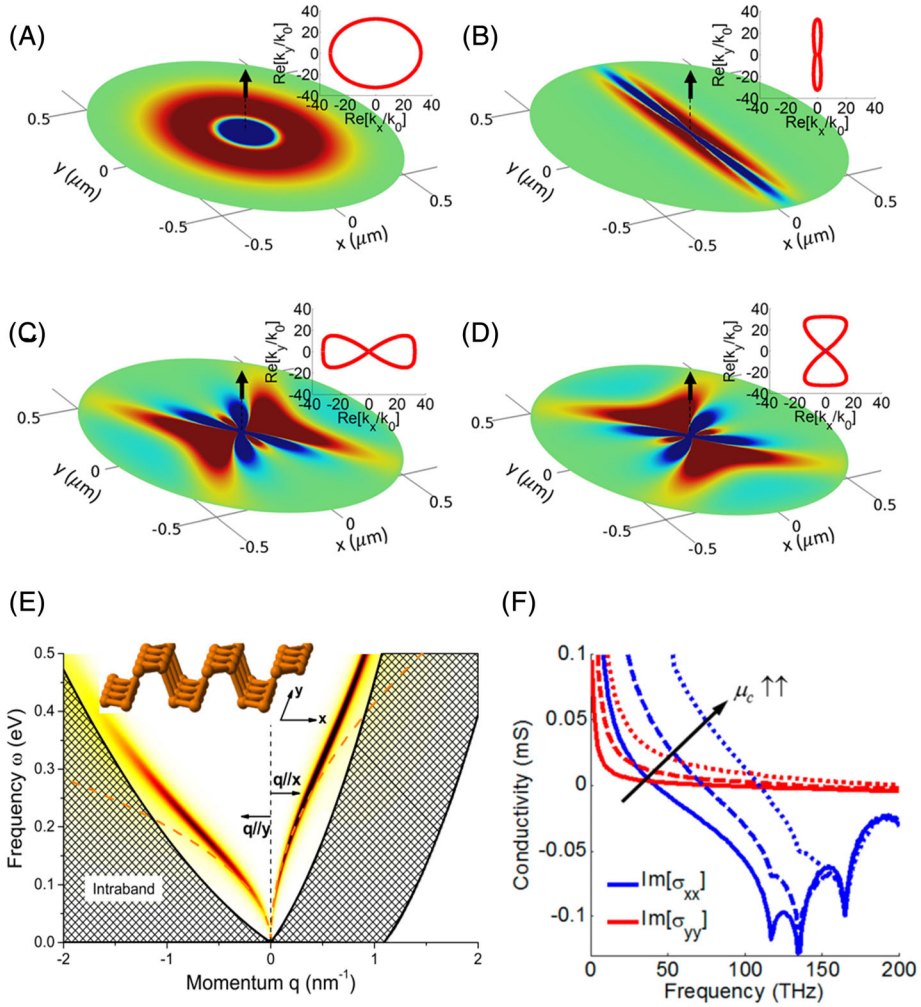

FIGURE 5 Theoretical investigation of in-plane anisotropic polaritons on planar surface.[4,29,100] A, dipole launched SPP along an isotropic surface. B, SPP along extremely anisotropic σ near-zero surface. C, SPP along hyperbolic surface (quasi-TM mode). D, SPP along hyperbolic surface (quasi-TE mode). Reproduced with permission from Reference 29 copyright 2015, American Chemical Society. E, BP plasmon dispersion along two in-plane directions. Reproduced with permission from Reference 4 copyright 2014, American Physical Society, F, in-plane anisotropic imaginary part of BP conductivity (real part of permittivity) vs frequency at different chemical potentials. Reproduced with permission from Reference 100 copyright 2016, American Chemical Society

PhPs exhibit elliptic and hyperbolic dispersions, respectively. More strikingly, the anisotropic polaritons in α-MoO_3 have ultra-long amplitude lifetimes (up to 20 pico-seconds), offering new opportunities for sub-wavelength planar device aiming at directional modulation of ultra-fast light-matter interactions (usually at femto-seconds or pico-seconds range).

Unlike the polaritons in graphene and hBN, the wavefront of the in-plane hyperbolic polaritons exhibit the particular shape in sharp contrast to concentric rings. The anomalous (concave) wavefronts can be launched by a silver antenna on top of the α-MoO_3 sheet (Figure 6I-L).[35] The exotic wavefronts further indicate strong optical anisotropy in α-MoO_3. The giant optical in-plane anisotropy in natural barium titanium sulfide ($BaTiS_3$) was also reported by Niu et al.[111] However, the in-plane anisotropic polaritons were not referred to in this work. The in-plane hyperbolic polaritons in van der Waals materials own the unusual features of hyperbolicity in bulk hyperbolic metamaterials, making it intriguing for exotic optical applications such as negative refraction,[20,21] hyperlens,[22-24] and enhancement of quantum radiation.[27] Most importantly, all these phenomena are realized in a planar surface rather than complicated structures, rendering easier accessibility.

Although the anisotropic plasmon polaritons have not been experimentally observed in intrinsic BP, the anisotropic dispersion in BP can be utilized to modulate the in-plane polaritons in hBN by constructing a vertical heterostructure of BP and hBN. The PhPs in hBN

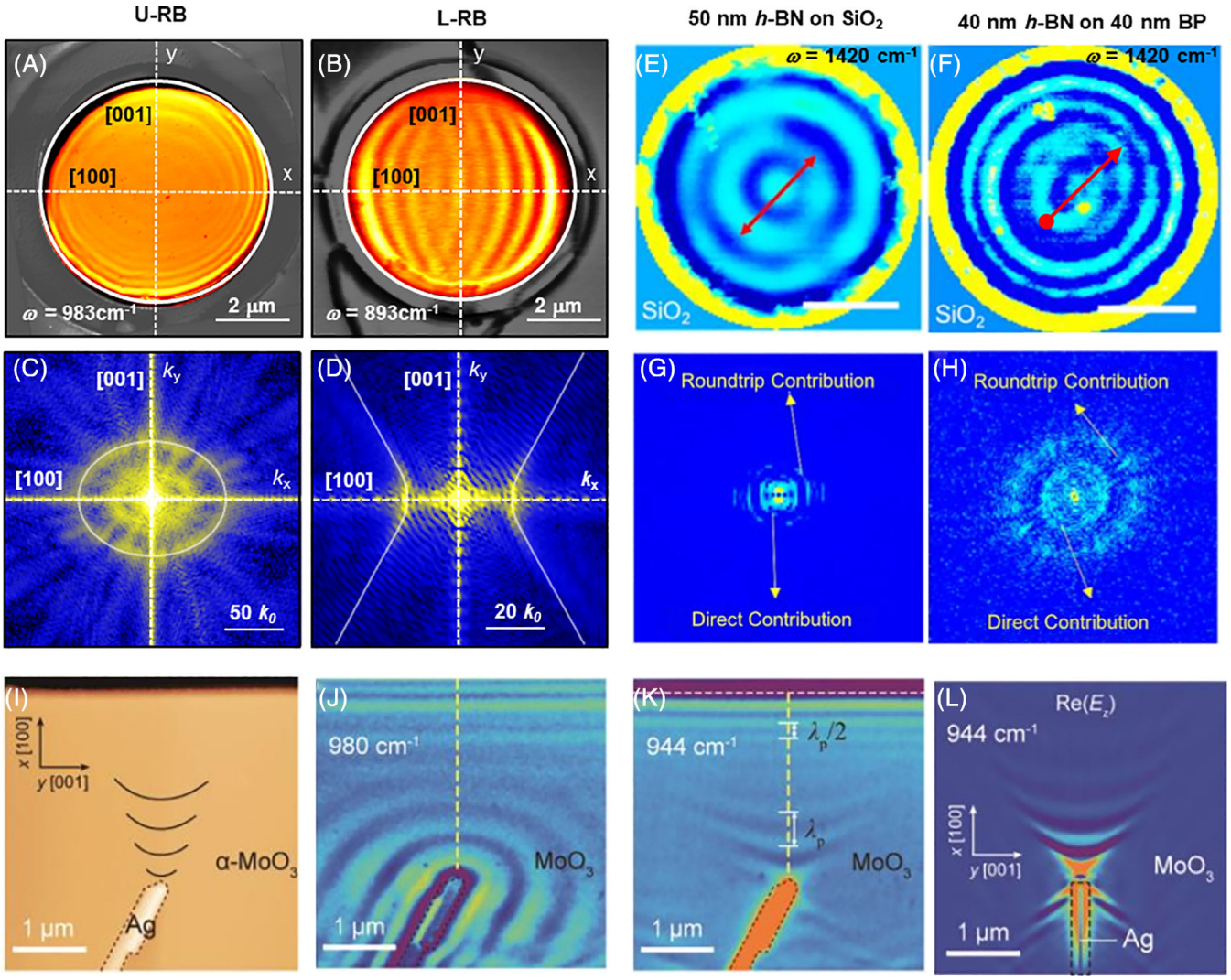

FIGURE 6 Near-field experimental horizon of polaritons in naturally in-plane anisotropic materials.[34,35,110] A, s-SNOM image of in-plane elliptical PhPs in an α-MoO_3 disk in upper RB. B, s-SNOM image of in-plane hyperbolic PhPs in an α-MoO_3 disk in lower RB. C and D, Absolute value of the Fourier transform of the near-field images in A and B respectively, revealing the iso-frequency contours of ellipse and hyperbola for each RB. Reproduced with permission from Reference 34 copyright, Nature Publishing Group. E, s-SNOM image of pure isotropic PhPs in hBN. F, s-SNOM image of PhPs in hBN/BP heterostructure. Scale bars are 2 μm. G and H, Fourier transform of the near-field images in e and f respectively, direct contribution and round-trip contribution represent the tip-launched and edge-launched PhPs here. From Reference 110 reprinted with permission from AAAS. I, Topography of silver antenna placed onto α-MoO_3 surface. J and K, In-plane elliptical and hyperbolic wavefront, respectively. L, Numerical simulations of s-SNOM image in K. From Reference 35 reprinted with permission from AAAS. BP, black phosphorus; hBN, hexagonal boron nitride; PhPs, phonon polaritons; s-SNOM, scattering-type scanning near-field optical microscopy

have prompted intensive investigations on the low-loss and volume-bound nature of hyperbolic PhP modes. Nevertheless, the intrinsic PhPs in hBN normally propagate as a cylindrical wave in hBN sheet, manifesting as in-plane isotropic nature. However, the propagation behavior of polaritons in hBN will be modified while a piece of hBN disk is placed on top of a piece of BP nanosheet. In particular, anisotropic polaritonic modes can be observed along zigzag and armchair axes of BP, as shown in Figure 6E-H.[110] More specifically, the nanoimaging results show characteristic elliptical interferometry pattern in hBN/BP heterostructure (Figure 6F) in contrast with an concentric pattern in pure hBN (Figure 6E). This could be a general approach to achieve tailored anisotropic optical properties by stacking two van der Waals materials with different optical birefringencies to form a new metasurface. From point of view of polaritonic regime, longitudinal optical phonon-plasmon coupling effect could also be another way to modulate the anisotropic properties of polar semiconductor.[105,112]

6 | CONCLUSIONS AND OUTLOOK

In this review, we briefly reviewed the recent progress of the 2D polaritonic materials. Particular attention is paid to natural van der Waals materials that have in-plane optical anisotropy in terms of anisotropic dispersion, which enables anisotropic phonon or plasmon polaritons. Inspired by the mechanisms for optical in-plane anisotropy, that is, the interplay between anisotropic electron motions can support anisotropic surface plasmon, this concept could also be generalized for other materials with similar structure as BP, for example, semimetals like $MoTe_2$, WTe_2.[113,114] On the other hand, similar to α-MoO_3, anisotropic crystals such as V_2O_5[115] and WO_3[116] are also potential candidates to support anisotropic propagation of polaritons. It is worth mentioning here that external parameters like pressure and doping can tune the materials properties as well and therefore their implements in polaritonics or plasmonics will further enrich our basic understanding of underlying physical phenomenas, which can stimulate more fundamental or technological breakthroughs for practical nanophotonic applications.

Compared with traditional metasurface, naturally anisotropic materials are not limited to the size of "meta-atom" which is corresponding to the maximum momentum of polaritons that can be supported. Such natural hyperbolicity could induce an extremely small wavelength, resulting in miniaturized optical devices for sensing, signal processing and quantum computing. Also, the use of natural materials can avoid time-consuming fabrication and eliminate the high inherent losses associated to fabrication processes. There is a great deal of polaritonics based on natural 2D materials, which are particularly suitable for the planar and directional light modulation with on-chip integration. Although the polaritonics of naturally in-plane hyperbolic materials is still an emerging research field, one can envision many distinctive phenomena such as planar negative refraction, waveguiding, hyperlensing, waveplate, and engineering of exotic wavefront of polaritons for the near future. Finally, the natural in-plane hyperbolic materials could open new possibilities for energy control and assist directional heat transfer with extreme efficiency.

ACKNOWLEDGMENTS

B.S. acknowledges the funding support from the China Postdoctoral Science Foundation Grant (No. 2017 M622758). Q. Bao acknowledges the support from the Australian Research Council (ARC, IH150100006, FT150100450, and CE170100039).

CONFLICT OF INTEREST

All the authors declare that they have no conflict of interest.

ORCID

Qingdong Ou https://orcid.org/0000-0003-2161-2543
Qiaoliang Bao https://orcid.org/0000-0002-6971-789X

REFERENCES

1. Chen J, Badioli M, Alonso-González P, et al. Optical nano-imaging of gate-tunable graphene plasmons. *Nature*. 2012; 487:77-81.
2. Fei Z, Rodin AS, Andreev GO, et al. Gate-tuning of graphene plasmons revealed by infrared nano-imaging. *Nature*. 2012; 487:82-85.
3. Ni GX, McLeod AS, Sun Z, et al. Fundamental limits to graphene plasmonics. *Nature*. 2018;557:530-533.
4. Low T, Roldán R, Wang H, et al. Plasmons and screening in monolayer and multilayer black phosphorus. *Phys Rev Lett*. 2014;113:106802.
5. Huber MA, Mooshammer F, Plankl M, et al. Femtosecond photo-switching of interface polaritons in black phosphorus heterostructures. *Nat Nanotechnol*. 2017;12:207-211.
6. Hu F, Luan Y, Scott ME, et al. Imaging exciton–polariton transport in $MoSe_2$ waveguides. *Nat Photon*. 2017;11:356-360.
7. Fei Z, Scott ME, Gosztola DJ, et al. Nano-optical imaging of WSe_2 waveguide modes revealing light-exciton interactions. *Phys Rev B*. 2016;94(8):081402.
8. Dufferwiel S, Schwarz S, Withers F, et al. Exciton–polaritons in van der Waals heterostructures embedded in tunable microcavities. *Nat Commun*. 2015;6:8579.
9. Dai S, Fei Z, Ma Q, et al. Tunable phonon polaritons in atomically thin van der Waals crystals of boron nitride. *Science*. 2014;343:1125-1129.
10. Caldwell JD, Kretinin AV, Chen Y, et al. Sub-diffractional volume-confined polaritons in the natural hyperbolic material hexagonal boron nitride. *Nat Commun*. 2014;5:5221.
11. Caldwell JD, Aharonovich I, Cassabois G, Edgar JH, Gil B, Basov DN. Photonics with hexagonal boron nitride. *Nat Rev Mater*. 2019;4:552-567.
12. Basov DN, Fogler MM, García de Abajo FJ. Polaritons in van der Waals materials. *Science*. 2016;354: aag1992.
13. Low T, Chaves A, Caldwell JD, et al. Polaritons in layered two-dimensional materials. *Nat Mater*. 2017;16:182-194.
14. Giles AJ, Dai S, Vurgaftman I. et al. Ultralow-loss polaritons in isotopically pure boron nitride. *Nature Materials* 2017; 17, 134.
15. Narimanov EE, Kildishev AV. Naturally hyperbolic. *Nat Photon*. 2015;9:214-216.
16. Hopfield J. Theory of the contribution of excitons to the complex dielectric constant of crystals. *Phys Rev*. 1958;112:1555-1567.
17. Newnham RE. *Properties of Materials: Anisotropy, Symmetry, Structure*. IN: Oxford University; 2005.
18. Gjerding MN, Petersen R, Pedersen TG, Mortensen NA, Thygesen KS. Layered van der Waals crystals with hyperbolic light dispersion. *Nat Commun*. 2017;8:320.
19. Poddubny A, Iorsh I, Belov P, Kivshar Y. Hyperbolic metamaterials. *Nat Photon*. 2013;7:948-957.
20. Hoffman AJ, Alekseyev L, Howard SS, et al. Negative refraction in semiconductor metamaterials. *Nat Mater*. 2007;6: 946-950.
21. Yao J, Liu Z, Liu Y, et al. Optical negative refraction in bulk metamaterials of nanowires. *Science*. 2008;321:930-930.

22. Liu Z, Lee H, Xiong Y, Sun C, Zhang X. Far-field optical hyperlens magnifying sub-diffraction-limited objects. *Science*. 2007;315:1686-1686.
23. Li P, Lewin M, Kretinin AV, et al. Hyperbolic phonon-polaritons in boron nitride for near-field optical imaging and focusing. *Nat Commun*. 2015;6:7507.
24. Dai S, Ma Q, Andersen T, et al. Subdiffractional focusing and guiding of polaritonic rays in a natural hyperbolic material. *Nat Commun*. 2015;6:6963.
25. Sun J, Xu T, Litchinitser NM. Experimental demonstration of demagnifying hyperlens. *Nano Lett*. 2016;16:7905-7909.
26. Xiong Y, Liu Z, Sun C, Zhang X. Two-dimensional imaging by far-field superlens at visible wavelengths. *Nano Lett*. 2007;7:3360-3365.
27. Noginov M A, Li H, Barnakov Y A. et al. Controlling spontaneous emission with metamaterials. *Optics Letters* 2010; 35, 1863-1865.
28. Ferrari L, Wu C, Lepage D, Zhang X, Liu Z. Hyperbolic metamaterials and their applications. *Prog Quantum Electron*. 2015;40:1-40.
29. Gomez-Diaz JS, Tymchenko M, Alu A. Hyperbolic plasmons and topological transitions over uniaxial metasurfaces. *Phys Rev Lett*. 2015;114:233901.
30. Sun Z, Gutiérrez-Rubio Á, Basov DN, Fogler MM. Hamiltonian optics of hyperbolic polaritons in nanogranules. *Nano Lett*. 2015;15:4455-4460.
31. Yoxall E, Schnell M, Nikitin AY, et al. Direct observation of ultraslow hyperbolic polariton propagation with negative phase velocity. *Nat Photon*. 2015;9:674-678.
32. Dai S, Ma Q, Yang Y, et al. Efficiency of launching highly confined polaritons by infrared light incident on a hyperbolic material. *Nano Lett*. 2017;17:5285-5290.
33. Li P, Dolado I, Alfaro-Mozaz FJ, et al. Infrared hyperbolic metasurface based on nanostructured van der Waals materials. *Science*. 2018;359:892-896.
34. Ma W, Alonso-González P, Li S, et al. In-plane anisotropic and ultra-low-loss polaritons in a natural van der Waals crystal. *Nature*. 2018;562:557-562.
35. Zheng Z, Xu N, Oscurato S L. et al. A mid-infrared biaxial hyperbolic van der Waals crystal. *Science Advances* 2019; 5, eaav8690.
36. Folland TG, Caldwell JD. Precise control of infrared polarization using crystal vibrations. *Nature*. 2018;562:499-501.
37. Gramotnev DK, Bozhevolnyi SI. Plasmonics beyond the diffraction limit. *Nat Photon*. 2010;4:83-91.
38. Barnes WL, Dereux A, Ebbesen TW. Surface plasmon subwavelength optics. *Nature*. 2003;424:824-830.
39. Atwater HA, Polman A. Plasmonics for improved photovoltaic devices. *Nat Mater*. 2010;9:205-213.
40. Kumar K, Duan H, Hegde RS, Koh SCW, Wei JN, Yang JKW. Printing colour at the optical diffraction limit. *Nat Nanotechnol*. 2012;7:557-561.
41. Boltasseva A, Atwater HA. Low-loss plasmonic metamaterials. *Science*. 2011;331:290-291.
42. Khurgin JB, Sun G. In search of the elusive lossless metal. *Appl Phys Lett*. 2010;96:181102.
43. Chen X, Hu D, Mescall R. et al. Modern Scattering-Type Scanning Near-Field Optical Microscopy for Advanced Material Research. *Advanced Materials* 2019; 31, 1804774.
44. Keilmann F, Hillenbrand R. Near-field microscopy by elastic light scattering from a tip. *Phil Trans R Soc Lond A*. 2004;362:787-805.
45. Brehm M, Taubner T, Hillenbrand R, Keilmann F. Infrared spectroscopic mapping of single nanoparticles and viruses at nanoscale resolution. *Nano Lett*. 2006;6:1307-1310.
46. Huth F, Schnell M, Wittborn J, Ocelic N, Hillenbrand R. Infrared-spectroscopic nanoimaging with a thermal source. *Nat Mater*. 2011;10:352-356.
47. Huth F, Govyadinov A, Amarie S, Nuansing W, Keilmann F, Hillenbrand R. Nano-FTIR absorption spectroscopy of molecular fingerprints at 20 nm spatial resolution. *Nano Lett*. 2012;12:3973-3978.
48. Hermann P, Hoehl A, Patoka P, Huth F, Rühl E, Ulm G. Near-field imaging and nano-Fourier-transform infrared spectroscopy using broadband synchrotron radiation. *Opt Express*. 2013;21:2913-2919.
49. Dai S, Ma Q, Liu MK, et al. Graphene on hexagonal boron nitride as a tunable hyperbolic metamaterial. *Nat Nanotechnol*. 2015;10:682-686.
50. Dai S, Fang W, Rivera N, et al. Phonon polaritons in monolayers of hexagonal boron nitride. *Adv Mater*. 2019;31:1806603.
51. Kumar A, Low T, Fung KH, Avouris P, Fang NX. Tunable light–matter interaction and the role of hyperbolicity in graphene–hBN system. *Nano Lett*. 2015;15:3172-3180.
52. Caldwell JD, Vurgaftman I, Tischler JG, Glembocki OJ, Owrutsky JC, Reinecke TL. Atomic-scale photonic hybrids for mid-infrared and terahertz nanophotonics. *Nat Nanotechnol*. 2016;11:9-15.
53. Woessner A, Lundeberg M B, Gao Y. et al. Highly confined low-loss plasmons in graphene–boron nitride heterostructures. *Nature Materials* 2014; 14, 421.
54. Brar VW, Jang MS, Sherrott M, et al. Hybrid surface-phonon-plasmon polariton modes in graphene/monolayer h-BN heterostructures. *Nano Lett*. 2014;14:3876-3880.
55. Jia Y, Zhao H, Guo Q, Wang X, Wang H, & Xia F. Tunable Plasmon–Phonon Polaritons in Layered Graphene–Hexagonal Boron Nitride Heterostructures. *ACS Photonics* 2015; 2, 907-912.
56. Yang X, Zhai F, Hu H, et al. Far-field spectroscopy and near-field optical imaging of coupled plasmon–phonon polaritons in 2D van der Waals heterostructures. *Adv Mater.* 2016;28:2931-2938.
57. Sunku SS, Ni GX, Jiang BY, et al. Photonic crystals for nano-light in moiré graphene superlattices. *Science*. 2018;362:1153-1156.
58. Zhang N, Surrente A, Baranowski M, et al. Moiré intralayer excitons in a $MoSe_2/MoS_2$ heterostructure. *Nano Lett*. 2018;18:7651-7657.
59. Ni GX, Wang H, Jiang BY. et al. Soliton superlattices in twisted hexagonal boron nitride. *Nature Communications* 2019; 10.
60. Ni GX, Wang L, Goldflam MD, et al. Ultrafast optical switching of infrared plasmon polaritons in high-mobility graphene. *Nat Photon*. 2016;10:244-247.
61. Dai S, Zhang J, Ma Q, et al. Phase-change hyperbolic heterostructures for nanopolaritonics: a case study of hBN/VO_2. *Adv Mater*. 2019;31:1900251.
62. Fali A, White ST, Folland TG, et al. Refractive index-based control of hyperbolic phonon-polariton propagation. *Nano Lett*. 2019;19:7725-7734.

63. Folland TG, Fali A, White ST, et al. Reconfigurable infrared hyperbolic metasurfaces using phase change materials. *Nat Commun*. 2018;9:4371.
64. Li P, Dolado I, Alfaro-Mozaz F J. et al. Optical nanoimaging of hyperbolic surface polaritons at the edges of van der Waals materials. *Nano Letters* 2016; 17, 228-235.
65. Zheng Z, Chen J, Wang Y, et al. Highly confined and tunable hyperbolic phonon polaritons in van der Waals semiconducting transition metal oxides. *Adv Mater*. 2018;30:1705318.
66. Mrejen M, Yadgarov L, Levanon A, Suchowski H. Transient exciton-polariton dynamics in WSe_2 by ultrafast near-field imaging. *Sci Adv*. 2019;5: eaat9618.
67. Hu D, Yang X, Li C, et al. Probing optical anisotropy of nanometer-thin van der waals microcrystals by near-field imaging. *Nat Commun*. 2017;8:1471.
68. Li L, Han W, Pi L, et al. Emerging in-plane anisotropic two-dimensional materials. *InfoMat*. 2019;1:54-73.
69. Zhang Q, Zhang R, Chen J, et al. Remarkable electronic and optical anisotropy of layered 1T'-WTe_2 2D materials. *Beilstein J Nanotechnol*. 2019;10:1745-1753.
70. Lu D, Liu Z. Hyperlenses and metalenses for far-field superresolution imaging. *Nat Commun*. 2012;3:1205.
71. Mohamed I, Pisano G, Ng MW. W-band Pancharatnam half-wave plate based on negative refractive index metamaterials. *Appl Optics*. 2014;53:2001-2006.
72. Zhang P, Ren P-L, Chen X-W. On the emission pattern of nanoscopic emitters in planar anisotropic matrix and nanoantenna structures. *Nanoscale*. 2019;11:11195-11201.
73. Kivshar Y, Rybin M. Anisotropy enables unusual waves. *Nat Photon*. 2017;11:212-214.
74. Sun J, Zhou J, Li B, Kang F. Indefinite permittivity and negative refraction in natural material: graphite. *Appl Phys Lett*. 2011;98:101901.
75. Guritanu V, Kuzmenko AB, van der Marel D, Kazakov SM, Zhigadlo ND, Karpinski J. Anisotropic optical conductivity and two colors of MgB_2. *Phys Rev B*. 2006;73:104509.
76. Estevâm da Silva R, Macêdo R, Dumelow T, da Costa JAP, Honorato SB, Ayala AP. Far-infrared slab lensing and subwavelength imaging in crystal quartz. *Phys Rev B*. 2012;86: 155152.
77. Esslinger M, Vogelgesang R, Talebi N, et al. Tetradymites as natural hyperbolic materials for the near-infrared to visible. *ACS Photon*. 2014;1:1285-1289.
78. Thompson DW, DeVries MJ, Tiwald TE, Woollam JA. Determination of optical anisotropy in calcite from ultraviolet to mid-infrared by generalized ellipsometry. *Thin Solid Films*. 1998;313-314:341-346.
79. Wang R, Sun J, Zhou J. Indefinite permittivity in uniaxial single crystal at infrared frequency. *Appl Phys Lett*. 2010;97: 031912.
80. Kildishev AV, Boltasseva A, Shalaev VM. Planar photonics with metasurfaces. *Science*. 2013;339:1232009.
81. Yu N, Capasso F. Flat optics with designer metasurfaces. *Nat Mater*. 2014;13:139-150.
82. Bilow HJ. Guided waves on a planar tensor impedance surface. *IEEE Trans Antennas Propag*. 2013;51:2788-2792.
83. Patel AM, Grbic A. Modeling and analysis of printed-circuit tensor impedance surfaces. *IEEE Trans Antennas Propag*. 2013;61:211-220.
84. Quarfoth R, Sievenpiper D. Artificial tensor impedance surface waveguides. *IEEE Trans Antennas Propag*. 2013;61:3597-3606.
85. Alonso-González P, Nikitin AY, Golmar F. et al. Controlling graphene plasmons with resonant metal antennas and spatial conductivity patterns. *Science* 2014; 344, 1369-1373.
86. Duan J, Chen R, Li J, Jin K, Sun Z, Chen J. Launching phonon polaritons by natural boron nitride wrinkles with modifiable dispersion by dielectric environments. *Adv Mater*. 2017; 29:1702494.
87. Huber A, Ocelic N, Kazantsev D, Hillenbrand R. Near-field imaging of mid-infrared surface phonon polariton propagation. *Appl Phys Lett*. 2005;87:081103.
88. Liu Y, Zhang X. Metasurfaces for manipulating surface plasmons. *Appl Phys Lett*. 2013;103:141101.
89. High AA, Devlin RC, Dibos A, et al. Visible-frequency hyperbolic metasurface. *Nature*. 2015;522:192-196.
90. Kapitanova PV, Ginzburg P, Rodríguez-Fortuño FJ, et al. Photonic spin hall effect in hyperbolic metamaterials for polarization-controlled routing of subwavelength modes. *Nat Commun*. 2014;5:3226.
91. Gomez-Diaz JS, Tymchenko M, Alù A. Hyperbolic metasurfaces: surface plasmons, light-matter interactions, and physical implementation using graphene strips. *Opt Mater Express*. 2015;5:2313-2329.
92. Huo P, Zhang S, Liang Y, Lu Y, Xu T. Hyperbolic metamaterials and metasurfaces: fundamentals and applications. *Adv Optic Mater*. 2019;**7**(14):1801616.
93. Xia F, Wang H, Xiao D, Dubey M, Ramasubramaniam A. Two-dimensional material nanophotonics. *Nat Photon*. 2014; 8:899-907.
94. Tan C, Cao X, Wu XJ, et al. Recent advances in ultrathin two-dimensional nanomaterials. *Chem Rev*. 2017;117:6225-6331.
95. Wang C, Zhang G, Huang S, Xie Y, Yan H. The optical properties and plasmonics of anisotropic 2D materials. *Adv Optic Mater*. 2019;**8**(5):1900996.
96. D'yakonov M. New type of electromagnetic wave propagating at an interface. *Sov Phys JETP*. 1988;67:714-716.
97. Narimanov EE. Dyakonov waves in biaxial anisotropic crystals. *Phys Rev A*. 2018;98:013818.
98. Lajaunie L, Boucher F, Dessapt R, Moreau P. Strong anisotropic influence of local-field effects on the dielectric response of α-MoO_3. *Phys Rev B*. 2013;88:115141.
99. Correas-Serrano D, Gomez-Diaz J, Melcon AA, Alù A. Black phosphorus plasmonics: anisotropic elliptical propagation and nonlocality-induced canalization. *J Optics*. 2016;18:104006.
100. Lee I-H, Martin-Moreno L, Mohr DA, Khaliji K, Low T, Oh SH. Anisotropic acoustic plasmons in black phosphorus. *ACS Photon*. 2018;5:2208-2216.
101. Nemilentsau A, Low T, Hanson G. Anisotropic 2D materials for tunable hyperbolic plasmonics. *Phys Rev Lett*. 2016;116:066804.
102. Gomez-Diaz J, Alu A. Flatland optics with hyperbolic metasurfaces. *ACS Photon*. 2016;3:2211-2224.
103. Nemilentsau A, Stauber T, Gómez-Santos G, Luskin M, Low T. Switchable and unidirectional plasmonic beacons in hyperbolic two-dimensional materials. *Phys Rev B*. 2019;99:201405.
104. Van Veen E, Nemilentsau A, Kumar A. et al. Tuning Two-Dimensional Hyperbolic Plasmons in Black Phosphorus. *Physical Review Applied* 2019; 12, 014011.

105. Dunkelberger AD, Ellis CT, Ratchford DC, et al. Active tuning of surface phonon polariton resonances via carrier photoinjection. *Nat Photon*. 2018;12:50-56.
106. Nicotra G, van Veen E, Deretzis I, et al. Anisotropic ultraviolet-plasmon dispersion in black phosphorus. *Nanoscale*. 2018;10:21918-21927.
107. Álvarez-Pérez G, Voronin KV, Volkov VS, Alonso-González P, Nikitin AY. Analytical approximations for the dispersion of electromagnetic modes in slabs of biaxial crystals. *Phys Rev B*. 2019;100:235408.
108. Álvarez-Pérez G, Folland T G, Errea I. et al. Infrared permittivity of the biaxial van der Waals semiconductor α-MoO3 from near-and far-field correlative studies. Arxiv preprint arXiv2019; 1912.06267.
109. Feng K, Streyer W, Zhong Y, Hoffman A, Wasserman D. Photonic materials, structures and devices for Reststrahlen optics. *Opt Express*. 2015;23:A1418-A1433.
110. Chaudhary K, Tamagnone M, Rezaee M, et al. Engineering phonon polaritons in van der Waals heterostructures to enhance in-plane optical anisotropy. *Sci Adv*. 2019;5:eaau7171.
111. Niu S, Joe G, Zhao H, et al. Giant optical anisotropy in a quasi-one-dimensional crystal. *Nat Photon*. 2018;12:392-396.
112. Spann BT, Compton R, Ratchford D, et al. Photoinduced tunability of the reststrahlen band in 4H-SiC. *Phys Rev B*. 2016;93:085205.
113. Soluyanov AA, Gresch D, Wang Z, et al. Type-ii weyl semimetals. *Nature*. 2015;527:495-498.
114. Huang L, McCormick TM, Ochi M, et al. Spectroscopic evidence for a type II Weyl semimetallic state in $MoTe_2$. *Nat Mater*. 2016;15:1155-1160.
115. Bhandari C, Lambrecht WR. Phonons and related spectra in bulk and monolayer V_2O_5. *Phys Rev B*. 2014;89:045109.
116. Chemseddine A, Babonneau F, Livage J. Anisotropic $WO_3 \cdot nH_2O$ layers deposited from gels. *J Non Cryst Solids*. 1987;91:271-278.

AUTHOR BIOGRAPHIES

Weiliang Ma is currently a research assistant in Optoelectronics and School of Optical and Electronic Information, Huazhong University of Science and Technology, China. He received her BSc and MSc both in physics from Soochow University, Suzhou, China in 2015 and 2018. His main research interests are 2D materials and nanophotonics.

Babar Shabbir is currently a research fellow at Department of Material Science and Engineering, Monash University. In 2016, Babar graduated from University of Wollongong, Australia with a PhD in physics. Before that, he graduated with MSc (2006) and MPhil (2009) in physics from Quaid I Azam University, Pakistan. His research area is two-dimensional materials with a particular focus on light matter interaction applications.

Qiaoliang Bao received his BA (2000) and ME (2003) degrees in Materials Science and Engineering from Wuhan University of Technology (China). He obtained his PhD degree (2007) in Materials Physics and Chemistry from Wuhan University (China). He worked as postdoctoral fellow at Nanyang Technological University and National University of Singapore from 2007 to 2012. He was appointed as a tenured associate professor at Department of Materials Science and Engineering, Monash University in 2016. His research interests include waveguide-coupled 2D semiconductors and polariton-coupled 2D materials and devices, focusing on the effect of confined-space light-matter interactions on the transport of electrons or other quasi-particles such as plasmon polariton, exciton polarition, and phonon polariton.

How to cite this article: Ma W, Shabbir B, Ou Q, et al. Anisotropic polaritons in van der Waals materials. *InfoMat*. 2020;1–14. https://doi.org/10.1002/inf2.12119